9

Embedding Multiple Wires Within a Single TLM Node

K. Biwojno, P. Sewell, Y. Liu, and C. Christopoulos

The School of Electrical and Electronic Engineering, George Green Institute for Electromagnetics Research, The University of Nottingham, University Park, Nottingham NG7 2RD, UK

Abstract: Transmission Line Modelling, TLM, is an established technique for simulating electromagnetic fields in a wide variety of application areas. As with any numerical algorithm, the complexity of the problem that can be practically dealt with is determined by the availability of computational resources.

Particularly demanding of resources are simulations that involve a diverse range of physical scales, all of which have a discernable impact on the results of the simulation and which therefore must be adequately modelled. One recurring illustration of this, typical of EMC predictions, is the inclusion of thin wires in simulations of large-scale objects and where a significant volume of empty space must be modelled.

Previously, a specific TLM node has been developed that allows a single thin wire to be analytically embedded within one of the TLM nodes; centrally in 3D and arbitrarily placed in 2D. In this work we extend this formulation to provide a 2D TLM node that can include an arbitrary number of arbitrarily placed thin wires within one cell and which are coupled by their near fields. This is of particular interest for simulating cabling looms as well as for consideration of certain classes of micro-structured materials.

9.1 Introduction

Modeling for electromagnetic compatibility (EMC) requires dealing with systems that are both electrically large and yet contain small-scale features that significantly affect the overall behavior. The epitome of this scenario is the integration of thin wires into numerical simulations of large-scale objects separated, or surrounded, by a significant volume of empty space. Transmission line modeling (TLM) is a full wave numerical electromagnetic simulation method,[1] which offers both ease of use and flexibility and is, therefore, often applied to such EMC problems. Although, in principle, the use of fine meshing and multi-gridding techniques are possible with TLM, in practice, these can result in excessive storage and computational times in the above scenario. In an attempt to overcome these limitations, various special TLM approaches have been introduced to deal with thin wire structures, including the use of

separated or integrated solution procedures,[2] diakoptic techniques,[3] and special, nonstandard wire node models.[4,5] However, in all cases, the wires are assumed to be straight and orientated along one of the Cartesian axes.

An alternative thin wire TLM model has recently been proposed, which embeds the known analytical solutions in the immediate vicinity of the wire within an individual TLM node. This approach has been found to be extremely accurate without incurring any additional computation overheads.[6–8] This model has also been extended to the case of offset wires, removing the restriction that wires must lie at the centre of the node,[9] so that the only remaining shortcoming of this technique is that it is only possible to model one wire in each TLM node, which precludes its use for wires in very close proximity or for the important case of wire bundles. In this paper, the extension to this case is presented. As before, the local field is represented as a superposition of analytical field solutions, which are then sampled on the link lines of the TLM node, resulting in second order accuracy and guaranteed stability. A number of practical examples are presented and validated against exact analytic solutions.

9.2 Theoretical Formulation

Consider an arbitrary number of infinitely long z-directed wires in close proximity so that they all lie within the scope of one TLM node. The TLM node has four link lines entering into it and upon which the voltages and currents represent the electric and magnetic fields. As the circuit quantities in the TLM node represent the fields in a closed volume of space, the required relationship between all the link line currents and voltages is of the form

$$\underline{I} = j\underline{\underline{Y}}\underline{V} = j\sum_{n=1}^{4} \underline{v}_n y_n \underline{v}_n^T, \quad \text{where } \underline{i}_n = j y_n \underline{v}_n \quad \text{and} \quad \underline{v}_m^T \underline{v}_n = \delta_{mn}$$

where the admittance matrix, $\underline{\underline{Y}}$, is Hermitian. The explicit construction of the admittance matrix from the set $\underline{v}_n$ requires identifying a set of four local solutions to Maxwell's equations whose magnetic and electric fields at the link line sample points satisfy $\underline{h}_n = y_n \underline{e}_n$.

The total field can be expressed as

$$E^T = E^i + \sum_{q=1} E_q^s$$

where E^i is an incident field and E_q^s represents the field scattered from the q^{th} wire. The field scattered from each wire can be analytically expressed in terms of Hankel functions centred upon its own local coordinate system, as shown in Figure 9.1.

$$E_q^s = \sum_{m=-\infty}^{\infty} e^{-jm\theta_q} H_m^{(2)}(kr_q) X_{qm}^s = \underline{f}_q^T \underline{X}_q^s, \quad \text{with } f_{qm} = e^{-jm\theta_q} H_m^{(2)}(kr_q)$$

where $k = \omega/c$, ω and c being the angular frequency and the speed of light *in vacuo*. Each component of this expansion can then be re-expressed in terms of the coordinate system of the p^{th} wire using the Bessel function summation

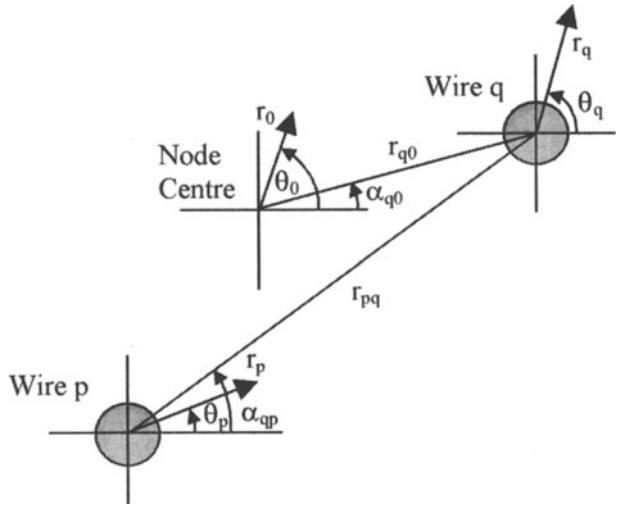

Figure 9.1 Notation used to describe the multi-wire TLM node. The wires are numbered from 1.

theorem.[10]

$$f_{qm} = e^{-jm\alpha_{qp}} \sum_{n=-\infty}^{\infty} J_n(kr_p) H^{(2)}_{m-n}(kr_{pq}) e^{jn\alpha_{qp}} e^{-jn\theta_p}$$

$$= \sum_{n=-\infty}^{\infty} e^{-jn\theta_p} J_n(kr_p) T_{pq_{mn}} = \underline{g}_p^T \underline{\underline{T}}_{pq_m}$$

where $g_{pn} = e^{-jn\theta_p} J_n(kr_p)$, so that $\underline{f}_q^T = \underline{g}_p^T \underline{\underline{T}}_{pq}$

Enforcing the vanishing of the total tangential electric on the surface of the p^{th} wire requires that

$$E^i + \underline{f}_p^T \underline{X}_p^s + \sum_{q \neq p} \underline{g}_p^T \underline{\underline{T}}_{pq} \underline{X}_q^s = 0 \qquad E^i = \sum_{m=-\infty}^{\infty} J_m(kr_0) e^{-jm\theta_0} X_{0m}^i = \underline{g}_0^T \underline{X}_0^i$$

where the incident field, E^i, has been defined in terms of the coordinate system centred on the node. E^i can be re-expressed in the coordinate system of the p^{th} wire using a matrix U, derived in the same manner as T above, i.e.,

$$J_m(kr_0)\, e^{-jm\theta_0} = e^{-jm\alpha_{0p}} \sum_{n=-\infty}^{\infty} J_n(kr_p) J_{m-n}(kr_{pq}) e^{jn\alpha_{0p}} e^{-jn\theta_p}$$

$$= \sum_{n=-\infty}^{\infty} e^{-jn\theta_p} J_n(kr_p) U_{p0_{mn}} = \underline{g}_p^T \underline{\underline{U}}_{p0_m}$$

Therefore, satisfaction of the boundary conditions on the wires requires that for all p

$$\underline{g}_p^T \underline{\underline{U}}_{p0} \underline{X}_0^i + \underline{f}_p^T \underline{X}_p^s + \sum_{q \neq p} \underline{g}_p^T \underline{\underline{T}}_{pq} \underline{X}_q^s = 0$$

which, for convenience, can be expressed as

$$\underline{\underline{U}}_{p0}\underline{X}_0^i + \underline{\underline{A}}_p\underline{X}_p^s + \sum_{q\neq p}\underline{\underline{T}}_{pq}\underline{X}_q^s = 0$$

where $\underline{\underline{A}}_p$ is a diagonal matrix of elements $H_m^{(2)}(ka_p)/J_m(ka_p)$, a_p being the radius of the p^{th} wire. This is a linear problem which can be solved for the scattering coefficients, $\underline{X}_p^s$, given the excitation coefficients $\underline{X}_0^i$. In general,

$$\underline{X}_p^s = \underline{\underline{M}}_p\underline{X}_0^i$$

To allow the mapping of the fields onto the TLM node, it is now necessary to express the total scattered field in the coordinate system centered on the node, which upon application of Green's theorems, is given by

$$E^s = \sum_{m=-\infty}^{\infty} H_m^{(2)}(kr_0)\, e^{-jm\phi_0} X_{0m}^s = \underline{f}_0^T \sum_p \underline{\underline{U}}_{p0}^H \underline{\underline{M}}_p \underline{X}_0 = \underline{\underline{N}}\,\underline{X}_0$$

Therefore, the total fields are given by

$$E^i + E^s = \left(\underline{g}_0^T + \underline{f}_0^T\underline{\underline{N}}\right)\underline{X}_0 \text{ and } -j\omega\mu(H^i + H^s) = \left(\frac{d\underline{g}_0^T}{dr} + \frac{d\underline{f}_0^T}{dr}\underline{\underline{N}}\right)\underline{X}_0$$

Now the eigenvalue problem discussed above can be imposed by requiring that the total electric field is proportional to the total magnetic field on the link lines, i.e., at $r = \Delta$ and $\phi_0 = 0$, $\pi/4$, π and $3\pi/4$, where Δ is half the nodal spacing. Therefore, we solve for the four lowest order eigensolutions of

$$\left(\frac{d\underline{g}_0^T}{dr} + \frac{d\underline{f}_0^T}{dr}\underline{\underline{N}}\right)\underline{X}_0 = y\left(\underline{g}_0^T + \underline{f}_0^T\underline{\underline{N}}\right)\underline{X}_0$$

Given the solutions of this problem and the corresponding electric and magnetic fields, the admittance relationship for the TLM circuit model is now constructed as described above.

9.3 Numerical Results

Before the full capability of the new multi-wire node is demonstrated, results for the special case of a single wire, centrally positioned within a node, are compared and validated against those from the TLM node specifically designed for this case[7] and the analytical solution. An infinitely long z-directed wire is placed in the x–y plane with perfect magnetic (open circuit) boundaries at the top and bottom of the calculation window and excited by an incident plane wave pulse polarized parallel to the wire, as shown in Figure 9.2.

The simulation parameters are: node size = 0.05 m, total mesh area 60 m × 60 m, and the wire radius $a = 0.00625$ m, $r = 0$ m and $\theta = 0°$, where r and $\theta$are the distance and angle from centre of the TLM cell, respectively.

Figure 9.3 shows the electric field observed at the point OP, placed either two or eight nodes in front of the wire to assess both the near and far field accuracy. The frequency is normalized to the maximum frequency in the TLM simulation. From the graph it is observed that the multi-wire node provides excellent accuracy over the normalised frequency range, even beyond the normalised

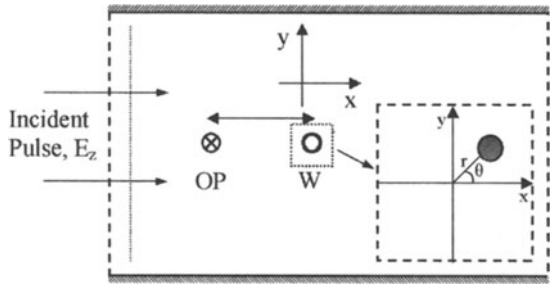

Figure 9.2 General test configuration: OP, observation point; W, – wire position.

frequency of 0.1, which is conventionally accepted to be the dispersion limit of TLM. Figure 9.4 presents the far field phase response of the field scattered from a wire for the same experiment.

The results presented so far indicate that the new multi-wire node can correctly model the single, centred wire case. To demonstrate its use with multiple wires an example with five wires of different radii and locations inside a single TLM node is examined. The simulation parameters are: mesh size = 0.05 m, total mesh area 60 m × 60 m, wire radii: $a_1 = 0.00625$ m, $a_2 = 0.003125$ m, $a_3 = 0.003$ m, $a_4 = 0.005$ m, $a_5 = 0.0075$ m, and the distances and angles from the centre of the node with reference to Figure 9.2 are: $r_1 = 0.0$ m, $r_2 = 0.0125$ m, $r_3 = 0.015$ m, $r_4 = 0.01625$ m, $a_5 = 0.015$ m, and $\theta_1 = 0°$, $\theta_2 = 30°$, $\theta_3 = 130°$, $\theta_4 = 225°$, $\theta_5 = 320°$, respectively.

Figures 9.5 and 9.6 show the amplitude of the total field and a phase of the scattered field for the five wires in a single TLM node. Clearly, the multi-wire technique can accurately model multiple wires with arbitrary placement within the cell and arbitrary radii, as very good agreement with theoretical results is observed.

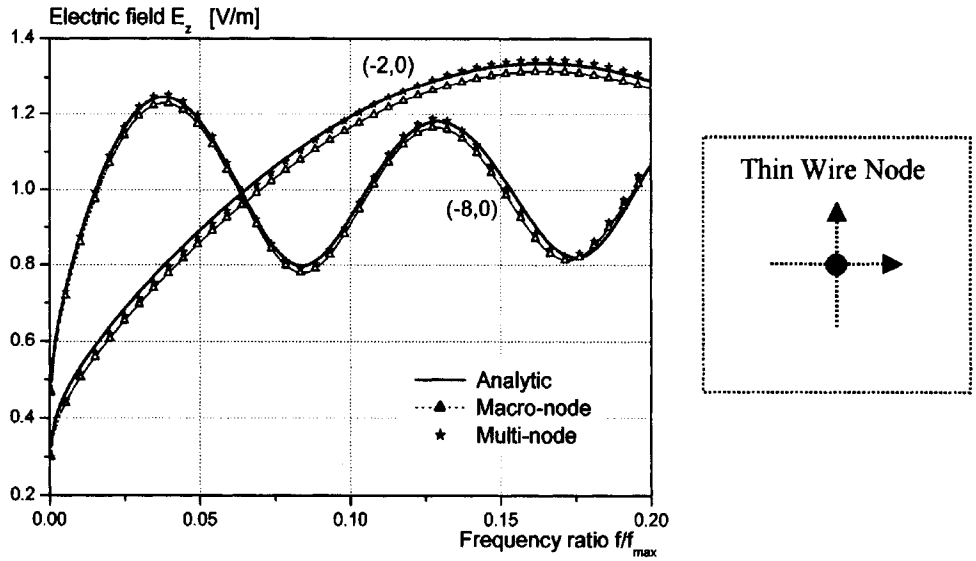

Figure 9.3 Magnitude of the electric field observed both two and eight nodes before a single centrally placed wire excited by a plane wave.

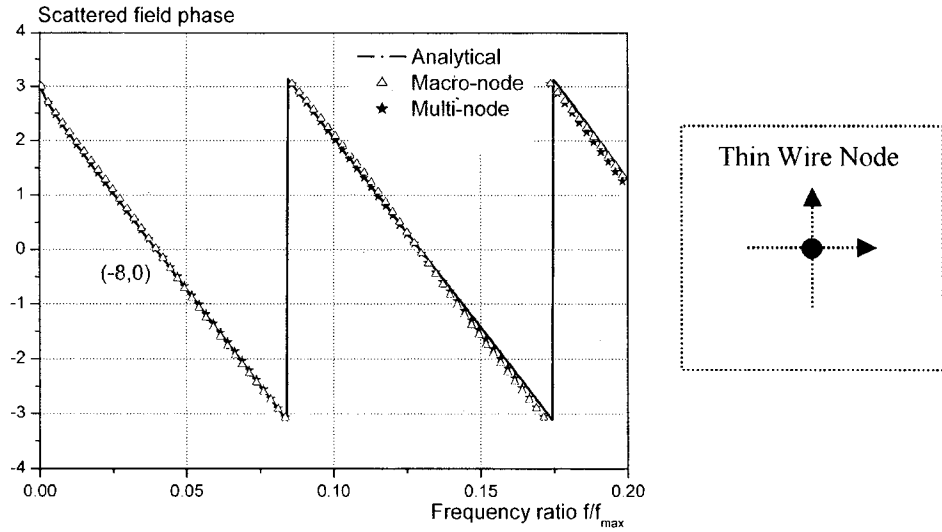

Figure 9.4 Phase of the electric field observed eight nodes before a single centrally placed wire excited by a plane wave.

The next two examples illustrate that the methodology developed above can also be modified to allow for more complex cylindrical scatterers. Specifically, small radii dielectric rods as well as dielectric coated conducting wires. Figure 9.7 shows the amplitude of the total electric field observed in front of two dielectric wires of the same radius $a = 0.00625$ m, placed in TLM cell at the same distances $r = 0.0125$ m from centre but at different angles $\theta_1 = 45°$ and $\theta_2 = -45°$, respectively, for two different values of permittivity.

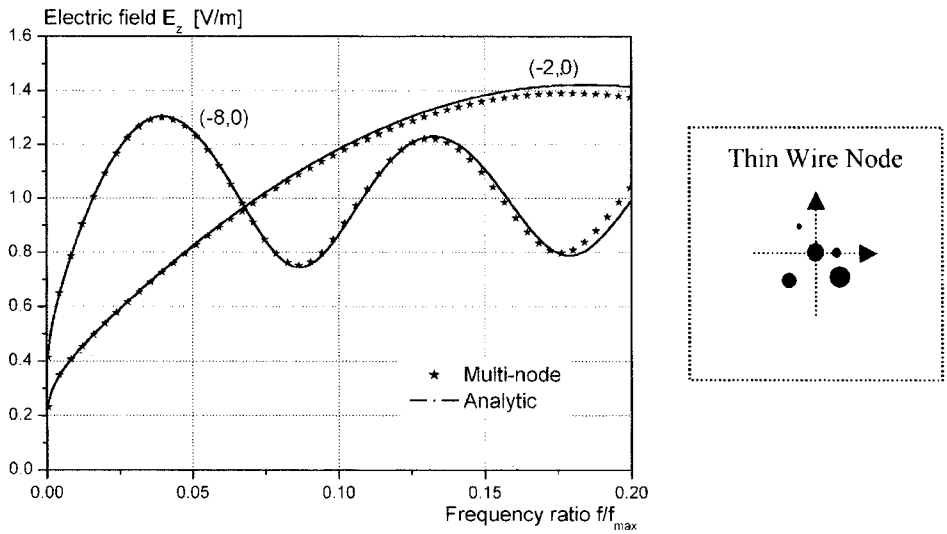

Figure 9.5 Magnitude of the electric field observed two and eight nodes in front of the node containing five wires when excited by a plane wave.

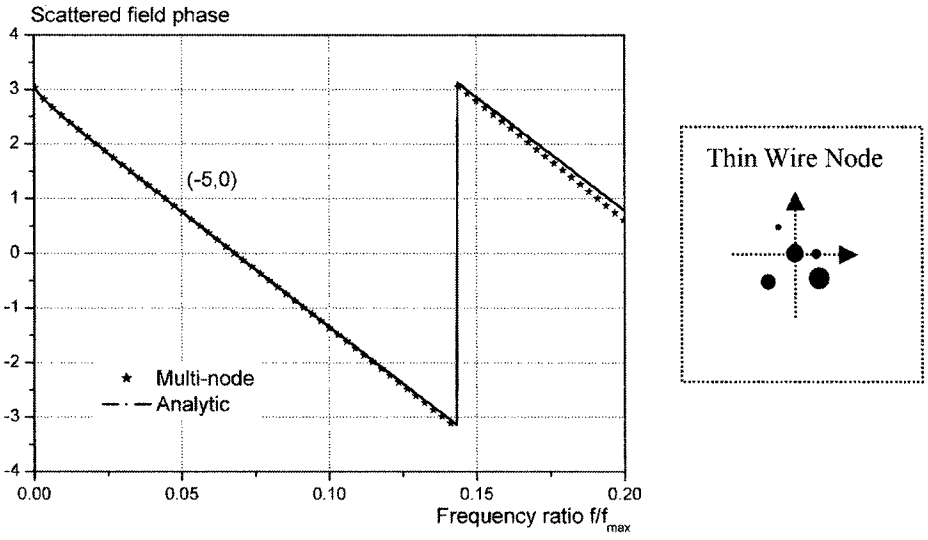

Figure 9.6 Phase of the electric field observed five nodes in front of the node containing five wires when excited by a plane wave.

Figure 9.8 shows the amplitude of electric field measured in front of three wires of radii $a_1 = 0.005$ m, $a_2 = 0.00625$ m, $a_3 = 0.0075$ m coated with dielectric relative permittivity 100 and radius $a = 0.0125$ m. The distances of wires from the centre of the cell are $r_1 = 0.01$ m, $r_2 = 0.01125$ m, $r_3 = 0.0125$ m and angles $\theta_1 = 45°$, $\theta_2 = -45°$, $\theta_3 = 180°$, respectively.

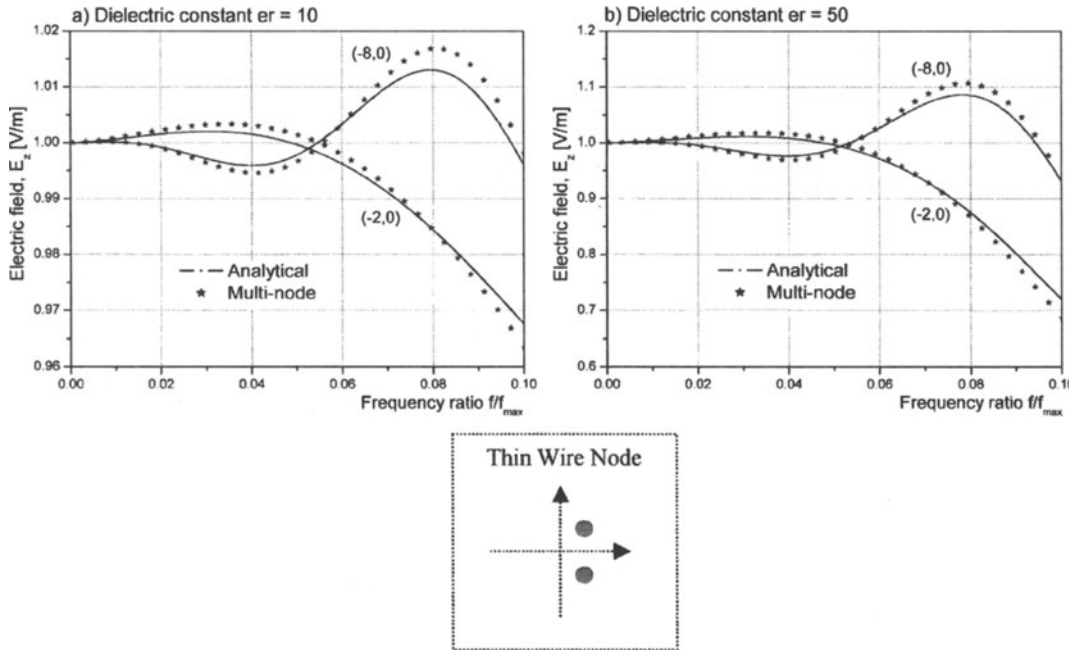

Figure 9.7 Magnitude of the electric field observed two and eight nodes in front of the node containing two dielectric wires when excited by a plane wave: a) $er = 10$ and b) $er = 50$.

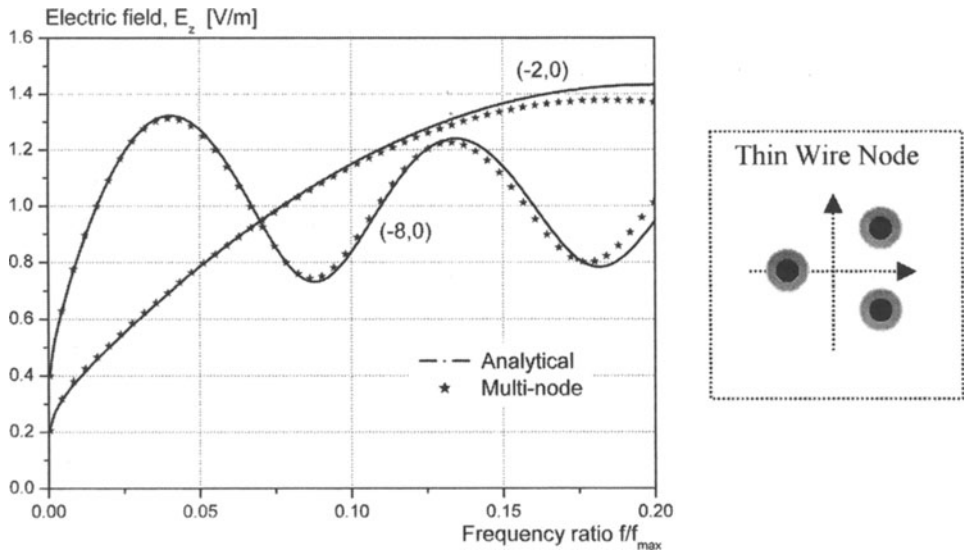

Figure 9.8 Magnitude of the electric field observed two and eight nodes in front of the node containing three dielectric coated wires when excited by a plane wave.

9.4 Conclusion

The high quality of the results presented above demonstrates that the multi-wire model has the ability to accurately integrate thin wires into a 2D TLM coarse mesh. There is no restriction on the number of wires, wire radii or their placement within a cell. The good accuracy of the results extends well beyond the frequency limit defined by requiring 10 nodes per wavelength. Finally, it has been shown that the approach easily extends to the case of dielectric rods or dielectric coated wires, and as no significant computational overhead is incurred, the new node is a powerful tool for numerical description of cabling looms and bundles or wire shields.

References

1. C. Christopoulos, *The Transmission-Line Modeling Method: TLM*, IEEE Press, New York, 1995.
2. P. Naylor, C. Christopoulos, and P. B. Johns, Coupling between electromagnetic field and wires using transmission-line modelling, in *Proceedings of the Inst. Electrical Engineering*, **134**, 1987, pp. 679–686.
3. P. B. Johns and K. Akhtarzad, The use of time domain diakoptics in time discrete models of fields, *Int. J. Numer. Methods Eng*, **17**, 1–14 (1981).
4. P. Naylor and C. Christopoulos, A new wire node for modelling thin wires in electromagnetic field problems solved by transmission line modelling, *IEEE Trans. Microw. Theory Technol.* **38**, 328–330 (1990).
5. A. J. Wlodarczyk and D. P. Johns, New wire interface for graded 3-D TLM, *Electron. Lett.* **28**, 728–729 (1992).
6. P. Sewell, Y. K. Choong, and C. Christopoulos, An accurate thin-wire model for 3D TLM simulations, *IEEE Trans. Electromag. Compat.*, **45**, 207–217 (2003).

7. Y. K. Choong, P. Sewell, and C. Christopoulos, Accurate modelling of an arbitrary placed thin wire in a coarse mesh, *IEEE Proc.- Sci., Meas. Technol.* **149**, 250–253 (2002).
8. Y. K. Choong, P. Sewell, and C. Christopoulos, New thin wire formulation for time-domain differential-equation models, *Int. J. Numer. Modelling*, **15**, 489–501 (2002).
9. Y. K. Choong, P. Sewell, and C. Christopoulos, Hybrid node for description of thin wires based on analytical field representation in EMC problems, in *IEEE 2002 International Symposiumon Electromagnetic Compatibility*, Minneapolis, Minnesota, USA, August 19–23, 2002.
10. I. S. Gradshteyn, I. M. Ryzhik, and Alan Jeffrey (eds.), *Table of Integrals, Series, and Products*, Academic Press, San Diego, CA, 1993, pp. 879.